

INTRODUCTION

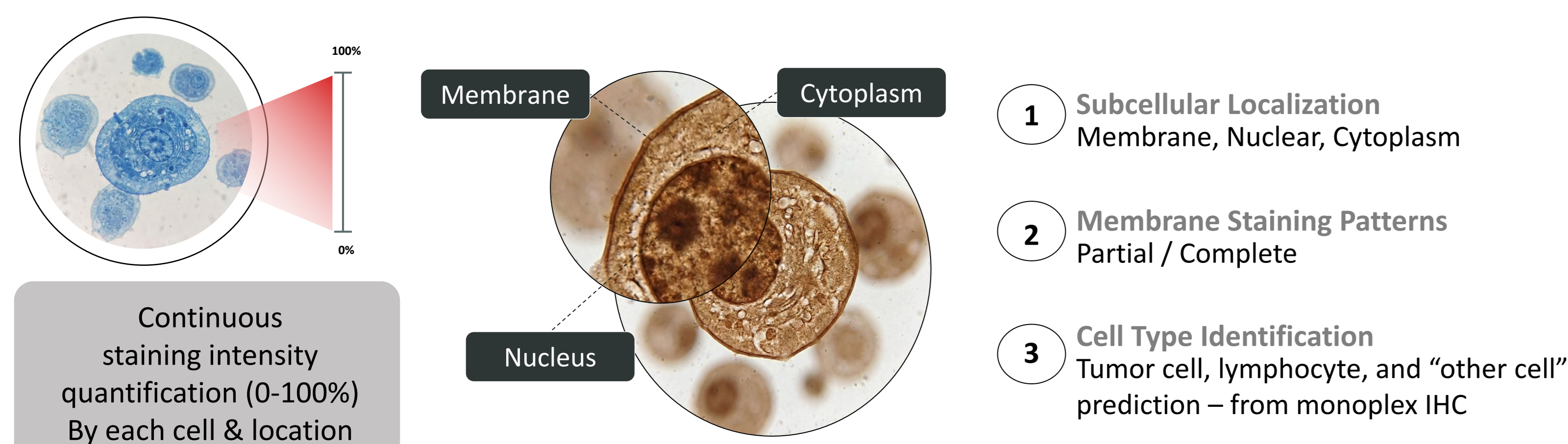
MET is a well-known oncogenic driver that confers various genomic aberrations. Recent approval of antibody-drug conjugates has expanded therapeutic options for c-MET expressing non-small cell lung cancer (NSCLC). However, the relationship between MET expression, tumor microenvironment (TME), and immunotherapy response remains unclear. This study explores the association between c-MET expression and spatial TME features in NSCLC to better understand its immunologic behavior.

METHODS

- **Study cohorts:** a total of 25,674 NSCLC samples across multiple cohorts
 - Genomic analysis: 24,110 samples from AACR GENIE and 924 samples from TCGA
 - IHC and TME analysis: 589 slides from Ajou University Medical Center (AUMC) and 51 slides from Agilent Technologies
- **AI-based Quantification:** Lunit SCOPE IO and Lunit SCOPE uIHC were used for quantitative assessment of TME and IHC-based c-MET expression (Figure 1).
- **IHC Analysis:** Lunit SCOPE uIHC quantified
 - 1) % Staining intensity ($\geq T1+$, $\geq T2+$, $\geq T3+$) & tumor cell proportion (scale 0–100)
 - 2) Subcellular compartment intensity (membrane, cytoplasm, nucleus)
- **Membrane-Specific Expression:**

$$\frac{\text{Membrane intensity}}{(\text{membrane} + \text{cytoplasm}) \text{ intensity}} \geq 0.5$$

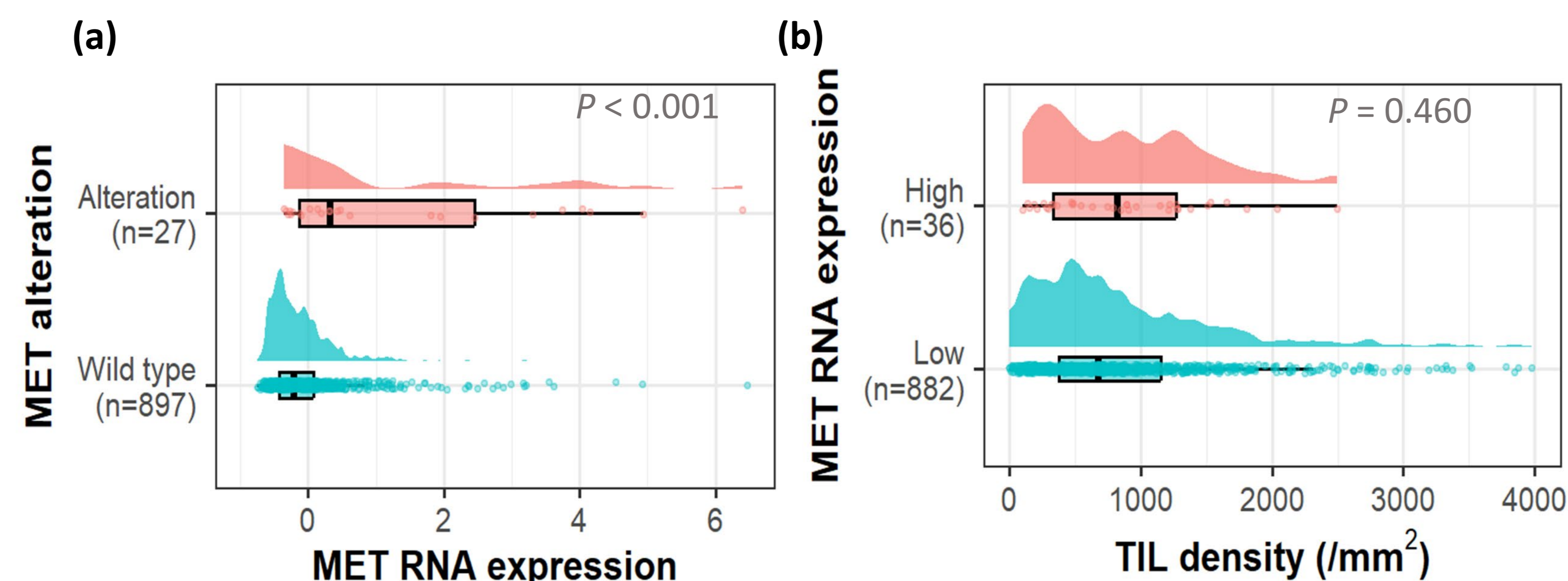
Figure 1. Overview of AI-powered Lunit universal IHC analysis. The AI model enables quantitative and spatial characterization of immunohistochemistry signals at single-cell resolution.



RESULTS

MET alterations occurred in 27 (2.9%) of TCGA and 909 (3.8%) of GENIE, including exon 14 skipping (n=388, 1.5%), amplification (n=380, 1.5%), and others (n=223, 0.9%). MET-altered tumors had higher MET RNA expression compared with wild-type tumors (median: 0.4 vs. -0.2, $p < 0.001$) (Figure 2a). TME analysis of samples with high and low RNA expression showed no significant difference in tumor-infiltrating lymphocyte (TIL) density (/mm², median: 851 vs. 673, $p = 0.46$) (Figure 2b).

Figure 2. MET alterations, RNA expression, and TIL density in TCGA and GENIE cohorts. High MET expression was defined as Z-score ≥ 2 ; TIL density was compared by expression level.

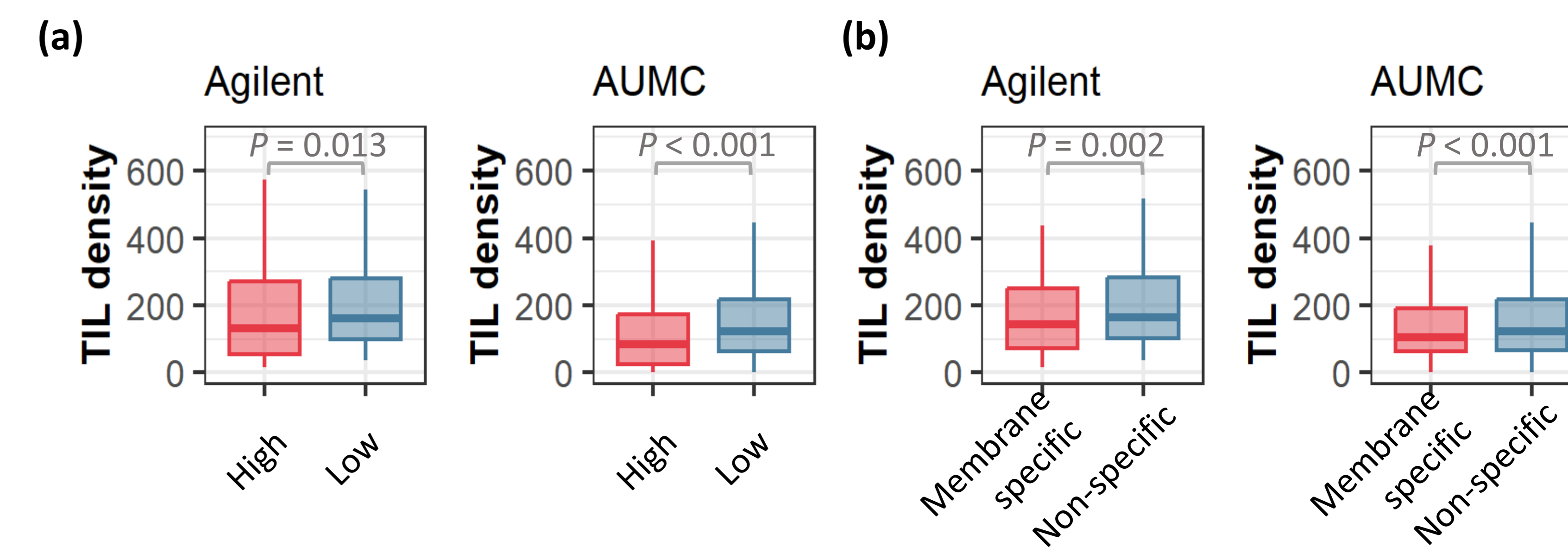


In 640 pairs of H&E and IHC slides from Agilent and AUMC, c-MET positive (T3+, $\geq 50\%$) samples showed numerically lower TIL density at the slide level compared to c-MET negative samples; however, this difference was not statistically significant (Agilent: median 80.6 vs. 211.3, $p = 0.229$; AUMC, 78.5 vs. 79.2, $p = 0.154$).

This trend became significant with cell and subcellular spatial analysis. The density of TIL was markedly reduced within 30 μ m of tumor cells exhibiting strong (3+) c-MET expression (median: 132.2 vs. 162, $p = 0.013$; 85.5 vs. 121.6, $p < 0.001$, respectively) (Figure 3a). Notably, a similar reduction in TIL density was also observed around tumor cells with membrane-specific c-MET expression (median: 144.9 vs. 165.8, $p = 0.002$; 106.6 vs. 122.3, $p < 0.001$, respectively) (Figure 3b).

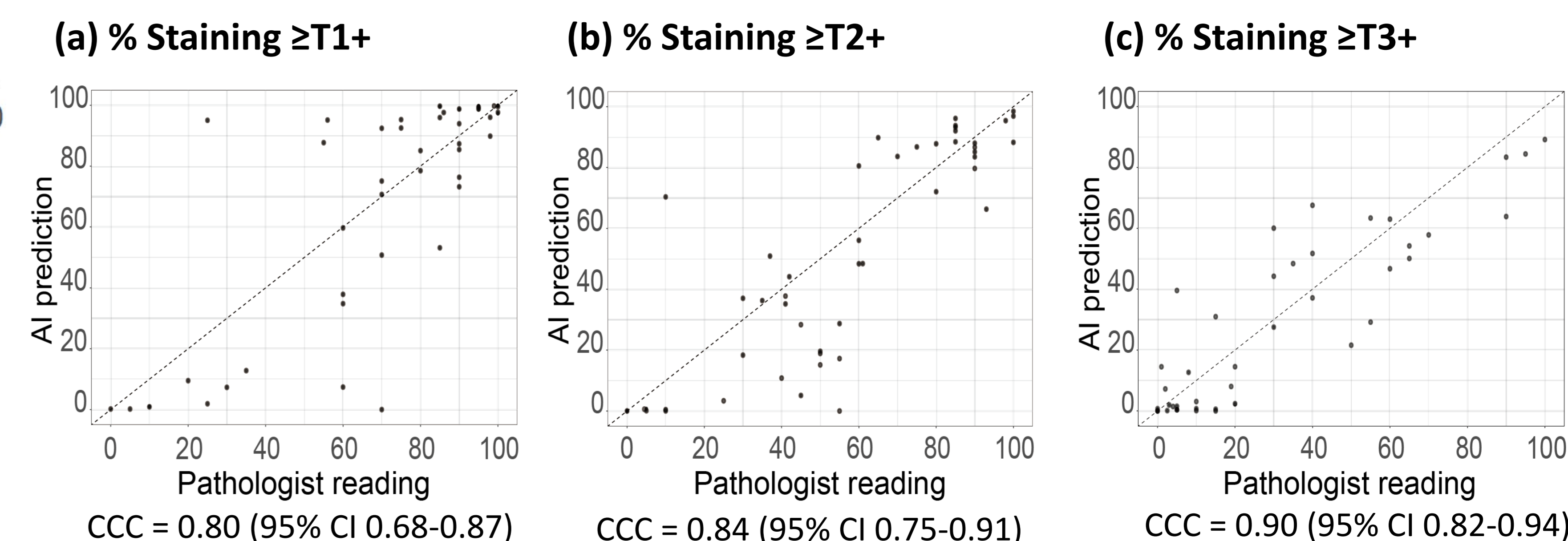
Figure 3. TIL density by c-MET expression patterns.

(a) TIL density according to c-MET IHC intensity (High vs. Low). (b) TIL density according to membrane-specific c-MET expression (membrane-specific vs. non-specific).



From the Agilent dataset, concordance between AI model-predicted and pathologist-assessed tumor cell proportions was evaluated. Alignment was observed across % staining intensity at $\geq T1+$ (Figure 4a), $\geq T2+$ (Figure 4b), and $\geq T3+$ (Figure 4c) scoring algorithms, with concordance correlation coefficients (CCC) ranging from 0.80 to 0.90.

Figure 4. Concordance between AI-predicted and pathologist-assessed tumor cell category proportions. (a–c) Scatter plots comparing AI and pathologist estimates of tumor cell proportions classified as % staining intensity at $\geq T1+$, $\geq T2+$, and $\geq T3+$, respectively.



CONCLUSION

- High or membrane-specific c-MET expression is associated with reduced immune cell infiltration, suggesting immune exclusion
- AI-derived tumor cell proportions demonstrates alignment with pathologist assessments in the subset of Agilent-provided samples.
- Findings support a spatial rationale for combination strategies with immunotherapy